2018 International Conference on Unmanned Aircraft Systems (ICUAS)
Dallas, TX, USA, June 12-15, 2018

Fixed-wing UAV with transitioning flight capabilities : Model-Based or Model-Free Control approach? A preliminary study.

Jacson M. O. Barth[1], Jean-Philippe Condomines[1], Murat Bronz[1], Leandro R. Lustosa[2]
Jean-Marc Moschetta[3], Cédric Join[4,6] and Michel Fliess[5,6]

***Abstract*— Transitioning vehicles experience three different flight phases during typical missions. The hovering and forward flight phases have been researched widely, however the transition phase in between is more challenging and has been the subject of less research. One of the control approaches to handle the transition phase relies on model-based methods which require sophisticated wind-tunnel characterization. Accurate modeling of force and moments of a partially stalled wing and control surfaces is highly challenging and time consuming. In addition, these models usually require several flight measurements (such as angle of attack and low airspeed) that are difficult to obtain. As an alternative, some control approaches manage the transition phase without the need for sophisticated models. One example of such an approach is the Model Free Control (MFC). This paper compares the results obtained from both MFC and Linear Quadratic Regulator (LQR) applied to fixed-wing UAV with transitioning flight capability during hovering, transition and forward flight modes. Both of the controllers are designed for a transitioning vehicle called *MAVion*. The simulation results demonstrated that MFC increases the stability of the aircraft, especially in disturbed flight conditions.**

I. INTRODUCTION

The number and diversity of applications involving Micro Air Vehicles (MAVs) are extensive and have received a considerable attention in recent years. Among possible applications, different missions require the possibility of a take-off and landing from a small area. Rotary-wing configurations are more suitable for their vertical or short take-off and landing capabilities, however, fixed-wing configurations offer a better performance in terms of range, endurance and high-speed flight. On the other hand, Hybrid MAVs (HMAVs) are capable of performing efficient forward flight with the versatility of a rotary-wing vehicle for hovering applications, see Figure 1.

[1]Are with the UAV Systems Group, French Civil Aviation School, 31400 Toulouse, France. **[jacson-miguel.olszanecki-barth; jean-philippe.condomines; murat.bronz]@enac.fr**

[2]Is with the MIST Lab, École Polytechnique de Montréal, QC H3T 1J4, Canada. **leandro.lustosa@polymtl.ca**

[3]Is with the Department of Aerodynamics, Energetics and Propulsion, Institut Supérieur de l'Aéronautique et de l'Espace, 31400 Toulouse, France. **jean-marc.moschetta@isae-supaero.fr**

[4]Is with the CRAN (CNRS, UMR 7039)), Université de Lorraine, BP 239, 54506 Vandœuvre-lès-Nancy, France. **cedric.join@univ-lorraine.fr**

[5]Is with the LIX (CNRS, UMR 7161), École polytechnique, 91128 Palaiseau, France. **Michel.Fliess@polytechnique.edu**

[6]Are with the AL.I.E.N (Algèbre pour Identification & Estimation Numérique), 7 rue Maurice Barrès, 54330 Vézelise, France. **[michel.fliess; cedric.join]@alien-sas.com**

During transition phase maintaining constant altitude, HMAVs encounter very large angles of attack, often a partially stalled wing, and rapidly changing pitching moments [1]. Finding an effective control strategy is important in order to improve the flight performance and it remains an interesting challenge for the control community. In hover or forward flights, autopilots are able to stabilize MAV attitude by using linear controllers [2] and simple Proportional Integral Derivative (PID) control [3]. Although being simple to tune without the knowledge of the model, PID controllers are limited in terms of disturbance rejection [2][4]. Among the current techniques that are used to stabilize the Hybrid MAVs, nonlinear controls [5][6][7], and control laws based on "switching" [8][9] can be mentioned. However these are case-specific, and their adaptation to different models is a difficult task. HMAVs are usually classified as underactuated and highly non-linear systems. Therefore, defining an appropriate model structure that is both reliable in terms of aerodynamic interaction between propeller and wing, and that can also model post-stall intricacies effects, remains a complex work. Nevertheless, there are recent efforts validating a tail-sitter MAV model by wind tunnel campaign and experimental flight tests for the entire flight envelope [10][11][12]. These specific aerodynamic characteristics were computed to design a series of gain matrices which are then used in a scheduled Linear Quadratic Regulator [11]. However, modeling of the forces and moments at different airspeeds and different angles of attack is costly and time consuming, and not accessible easily by everyone.

Alternatively, a sensor-based approach called incremental

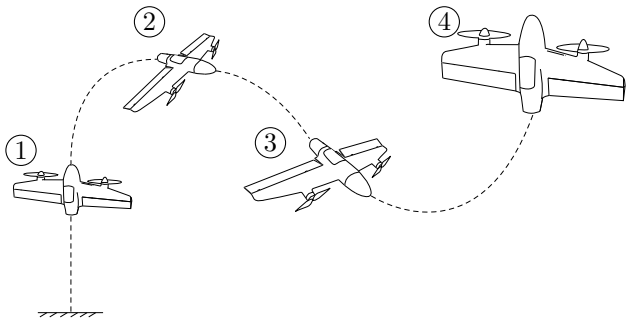

Fig. 1: Typical flight modes of Hybrid Micro Aerial Vehicles: 1 - Take-Off; 2 - Transition; 3 - Forward; 4 - Hover.

nonlinear dynamic inversion (INDI) which is less model-dependent and robust at disturbance rejection, was proposed [4][13]. This controller requires a sensor measurement to estimate a large part of the UAV model, except the actuator dynamics that must be characterized beforehand. By filtering and differentiating the gyroscope measurements, the angular acceleration is estimated, and an increment of the control input is calculated based on a desired increment in angular acceleration. Thus, disturbances as well as unmodeled dynamics are measured, computed and compensated. As a main drawback, INDI uses test flight data to tune off-line the control coefficients. *Of course, to do this, the MAV needs to be flying* [13], with predefined parameters.

The Model-Free Control term appears many times in the literature, but in distinct meanings from this paper. In fact, the growing importance of artificial intelligence and machine learning techniques, particularly through neural networks, has naturally been implanted into the model-free terms [14][15]. In this paper, we assume model-free control terms according to the simple algorithms proposed by [16][17] which have adaptive properties. MFC algorithms have been developed, and applied on MAVs providing a potential strategy for designing autopilots without considering any model [18][19][20][21][22]. Among them, nonlinear MFC strategy [20], has been applied in a nonlinear and strongly coupled system providing good performances in real flights with low computational costs which encourages its use in embedded systems. MFC guarantees a straightforward form of the tuning of the control loop which needs no modeling of the vehicle dynamics and is efficient at disturbance rejection. Whereas MFC approach can be viewed as a potential efficient method for dealing with post-stall phenomena, this model free based control has never been studied on HMAVs in pre-stall region and never compared with traditional approaches for transitioning fixed-wings. The main contributions of this paper are therefore :

- to make explicit (in §III-A and §III-B) the theoretical equations that describe both MFC and LQR controllers in the benchmarking case of the transitioning flight;
- to propose a novel preliminary comparative study (in §IV), focusing on transitioning flight, between traditional control methods and model free approach;

II. AERODYNAMIC PRELIMINARIES

Characterized by increased mission complexity, many innovative HMAVs are constantly emerging. These platforms may be divided into different groups: tilt-rotors [23], quadplanes [24] and tail-sitters or tilt-bodies [10][25][26]. Also, combination of the previous cited designs can be found, such as quad-tilt-rotors [27][28]. Quadplanes have independent propulsion systems for hovering and forward flight. Thus, the control laws can be optimized for each flight mode separately. By contrast, these configurations present more drag in cruise flight mode due to the additional quad-mechanical structure which does not always have optimized aerodynamic characteristics. In terms of endurance, tail-sitters are more promising. However, transition phase of tail-sitters include high angles of attack, and often a partially stalled wing and fast variations of pitching moment which increase the difficulty in modeling and control aspects [1].

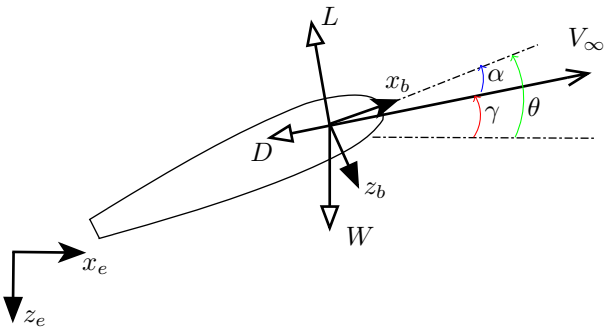

Fig. 2: Coordinate systems with vector forces and angles.

A. Coordinate system

In this paper we assume the same coordinate systems as a conventional fixed-wing aircraft. In Figure 2, the body frame denoted by (x_b, y_b, z_b) represents the front, right and down directions of the HMAV. Similarly, the inertial frame denoted by (x_e, y_e, z_e) describes the north, east and down directions. The HMAV orientations are defined by the attitude angles ϕ, θ, ψ, respectively, roll, pitch and yaw. Aerodynamic forces that act in the HMAV are described by lift (L) and the drag (D). The weight force is represented by the vector (W). In addition, the angle of attack (α) and the flight path angle (γ) which describes whether the aircraft is climbing or descending, can be seen in Figure 2.

B. Tail-sitter model

In this work, tail-sitter vehicle dynamics simulation is based on ϕ-theory [29] assumptions. The ϕ-theory framework for modeling aerodynamics allows us to write the differential equations of motion of the vehicle which specifications are presented in Table I, in the form

$$\dot{\boldsymbol{x}} = \gamma(\boldsymbol{x}, \boldsymbol{u}, \boldsymbol{w}) \tag{1}$$

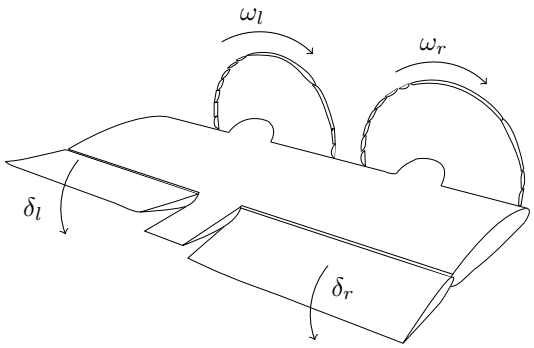

Fig. 3: A typical representation of the *MAVion* with our definitions of control inputs.

TABLE I: *MAVion* specifications.

Parameters	Values	SI Units
Mass	0.438	[Kg]
Mean Chord	0.21	[m]
Wingspan	0.42	[m]
Max Forward Speed	30	[m/s]
Wing Area	0.0882	$[m^2]$
I_{xx}	0.0036	[Kg m^2]
I_{yy}	0.0036	[Kg m^2]
I_{zz}	0.0072	[Kg m^2]

where $\boldsymbol{x} \in \mathbb{R}^{10}$, $\boldsymbol{u} \in \mathbb{R}^4$, $\boldsymbol{w} \in \mathbb{R}^3$ are, respectively, vehicle state, actuation inputs and wind disturbances, given by

$$\boldsymbol{x} = \begin{pmatrix} \boldsymbol{v}_l & \boldsymbol{\omega}_b & q \end{pmatrix}^T \tag{2}$$

and

$$\boldsymbol{u} = \begin{pmatrix} \omega_l & \omega_r & \delta_l & \delta_r \end{pmatrix}^T \tag{3}$$

In equation (2), $\boldsymbol{v}_l \in \mathbb{R}^3$, $\boldsymbol{\omega}_b \in \mathbb{R}^3$, $q \in \mathbb{R}^4$, denote respectively, vehicle velocity in local NED frame, angular velocity in body frame, and vehicle attitude. Each of the control inputs in $\boldsymbol{u}$ are defined according to Figure 3. The mathematical description of $\gamma(\cdot)$ is relatively intricate and, therefore, we refer the interested reader to [29] for further information. Nonetheless, we mention that $\gamma(\cdot)$ is an analytic continuous singularity-free formulation over a complete 360^o angle-of-attack and sideslip flight envelope, and therefore, control-engineering-friendly, in sharp contrast with other switched models or look-up-table-based methods present in the literature. Additionally, the model incorporates fundamental nonlinear aerodynamics effects – e.g., post-stall and propeller-induced prop-wash. Incidentally, the tilt-body nature of the vehicle calls for a global numerically stable formulation of attitude and justifies the use of quaternions.

III. THEORETICAL CONTROL BACKGROUND

Considering all the above mentioned, control laws used to stabilize the transition from hover to forward flight mode of HMAVs are, in most cases, based on the principle of "switching" between different control approaches. Here we propose, two global control methods: a scheduled LQR algorithm which is model-based and has the advantage of being simple to tune in MIMO systems; and a continuous adaptive controller, where no knowledge about the controlled system is required, called MFC. In our transition flight application, the choice to use such approach is due to the difficulty to derive a reliable and representative aerodynamic model for HMAVs.

A. Scheduled Linear Quadratic Regulator

For comparison purposes, we pursue a traditional full-state feedback scheduled-LQR control design, as previously done in [10]. LQR cost function gains are carefully chosen to accommodate for non-modeled effects of $\gamma(\cdot)$ in equation (1), e.g., discretization (bandwidth) of actuation inputs, wind disturbances and state estimation errors. For a given trim point the scheduled LQR computes a new matrix of gains K. As a result, it requires several gains to control the entire flight envelope (in the order of 10 matrix of gains, each one composed by 4 rows and 9 columns). An additional interesting point – although often overlooked or not commented in detail – is that quaternion-based nonlinear models linearization yields non-controllable linear models that preclude LQR control design. To overcome this issue we employ the virtual input strategy detailed in [30].

B. Model-free control approach

We present briefly the main theoretical principles of some research works dealing with on-line estimation and model-free control approach. Let's consider the following non linear state-space representation defined by :

$$\begin{cases} \dfrac{dx}{dt} = f(x,u) \\ y = h(x,u) \end{cases} \tag{4}$$

where $x(t)$, $u(t)$, $y(t)$ are the state, input and output vectors respectively. The output $y(t)$ is not directly available but rather it is observed through a noise corruption. A model for the output can be described by the following equation :

$$y_m(t) = y(t) + \omega(t) \tag{5}$$

where $\omega(t)$ is the observation noise. The exploitation of MFC principles requires the definition of a particular SISO model, named *Ultra-Local Model*, which corresponds to replace the unknown dynamic by a purely numerical model :

$$y_m^{(v)} = F + \alpha \cdot u \tag{6}$$

In equation (6), α is an element of $\mathbb{R}$ and is a non-physical constant parameter which allows us to define the same magnitude between $y_m^{(v)}$ and u. Moreover, the exploitation of this numerical model requires the knowledge of F. This quantity represents the real dynamics of the model as well as the different disturbances which could damage the output-system performances. Thus, an accurate estimation of F, defined as $\hat{F}$, is crucial and plays an import role in the MFC performance. Assuming that we do not know any model of the plant, its estimation can be calculated directly from measurements of y_m and u, with y_m corrupted by various noise sources provided from measurements devices.

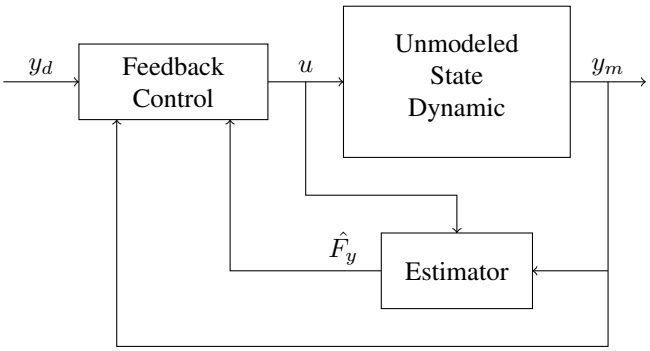

Fig. 4: Overall Model-Free Control schema.

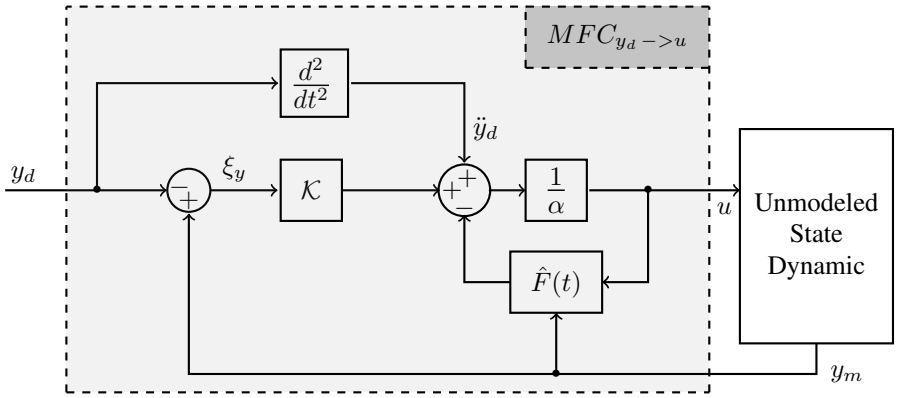

Fig. 5: Detailed Model-Free Control schema for a specific output dynamic y. Proportional-Derivative control $\mathcal{K}$. $\hat{F}(t)$ estimator of dynamic and disturbances and α a non-physical constant parameter.

Although significant work has been done on the development of derivative estimators such as [31] which uses recent algebraic identification techniques to estimate the derivative of noised measurements. We propose a simpler method that facilitates its implementation in real-time applications. Therefore, a suitable approximation of F in equation (6) is explained for the particular case of v = 1 and v = 2 using the classic *Laplace transform*. The following describe our proposed algorithm for a first-order dynamic estimation :

- For ($v = 1$), the *Ultra-Local Model* becomes :

$$\dot{y}_m = F + \alpha \cdot u \tag{7}$$

Referring to elementary operational calculus we transform the equation (7) to equation (8) :

$$sY_m(s) - y_m(0) = \frac{F}{s} + \alpha U(s) \tag{8}$$

Where $Y_m(s)$ and $U(s)$ corresponds to the *Laplace transforms* of y_m and u. By differentiating one the previous equations we are able to rid the initial condition $y_m(0)$:

$$s\frac{dY_m(s)}{ds} + Y_m(s) = -\frac{F}{s^2} + \alpha\frac{dU(s)}{ds} \tag{9}$$

However, s in the time domain corresponds to the derivation with respect to time and it is sensitive to noise corruptions. Therefore, in order to reduce both noise and numerical computation errors on the output estimation, we replace the derivative terms by integrators ($\frac{1}{s}$) who have robust properties with respect to noise. Thus, multiplying both sides of equation (9) by s^{-2}, we obtain :

$$\frac{dY_m(s)}{s\,ds} + \frac{Y_m(s)}{s^2} = -\frac{F}{s^4} + \frac{\alpha}{s^2}\frac{dU(s)}{ds} \tag{10}$$

Using inverse Laplace operator, equation (10) can be transferred back to the time domain employing convolution formula and classic *Inverse Laplace transforms* or *Cauchy's formula* to reduce multiple integrals in a simple one :

$$\hat{F} = \frac{-6}{T^3}\int_{t-T}^{t}[(T-2\sigma)y_m(\sigma) - \alpha\sigma(T-\sigma)u(\sigma)]d\sigma \tag{11}$$

Equation (11) estimates the dynamic of a first-order system from measurements of a corrupted signal (y_m). The result is a constant parameter $\hat{F}$ which is valid during the interval $[t-T, t]$. $\hat{F}$ is updated for each new sampling time and integral properties assure the attenuation of the noise.

- For ($v = 2$), the *Ultra-Local Model* becomes :

$$\ddot{y}_m = F + \alpha \cdot u \tag{12}$$

We apply exactly the same steps from equation (8) to equation (11). This time, for a second-order dynamic described in equation (12).

$$s^2Y_m(s) - sy_m(0) - \dot{y}_m(0) = \frac{F}{s} + \alpha U(s) \tag{13}$$

The initial condition is rid by differentiating twice the previous equation which leads to equation (14) :

$$2Y_m(s) + 4s\frac{dY_m(s)}{ds} + s^2\frac{d^2Y_m(s)}{ds^2} = \frac{2F}{s^3} + \alpha\frac{d^2U(s)}{ds^2} \tag{14}$$

The sensitivity to the noise generated by both differentiators s and s^2, is eliminated by adding integrators. Therefore, multiplying both sides of equation (14) by s^{-3} leads to equation (15).

$$\frac{2Y_m(s)}{s^3} + \frac{4}{s^2}\frac{dY_m(s)}{ds} + \frac{1}{s}\frac{d^2Y_m(s)}{ds^2} = \frac{2F}{s^6} + \frac{\alpha}{s^3}\frac{d^2U(s)}{ds^2} \tag{15}$$

Applying *Inverse Laplace transform*, we obtain the estimator ($\hat{F}$) for a second-order system represented in the time domain :

$$\hat{F} = \frac{5!}{2T^5}\int_{t-T}^{t}[(T-\sigma)^2 - 4\sigma(T-\sigma) + \sigma^2]y_m(\sigma)d\sigma - [\frac{\alpha}{2}\sigma^2(T-\sigma)^2u(\sigma)]d\sigma \tag{16}$$

Algorithm 1 $\hat{F}$ Estimator

1: **procedure**
2: $v \leftarrow$ Define estimator order
3: **step 1:** Write the *Ultra-Local Model*
4: **step 2:** Calculate the *Laplace transforms*
5: **step 3:** Derive step 2 v times with respect to s
6: **step 4:** Multiply the step 3 by $s^{-(v+1)}$
7: **step 5:** Calculate the *Inverse Laplace transforms*
8: **end procedure**;

The interval integration, with length T, corresponds to the window width of a receding horizon strategy. The choice of this quantity results in a trade-off. The idea is to choose the window width small so as to calculate the derivative estimate within an acceptable short delay but large enough in order to sustain the low pass filtering property for suppressing measurement noise on $y_m(t)$. Based on such estimator it is possible to design a model-free control estimating on-line the dynamic of $y(t)$ from a purely numerical model of the system.

The general form of the MFC architecture presented in Figure 4 and detailed in Figure 5 allows us to define the close-loop control such as :

$$u = \underbrace{-\frac{\hat{F}}{\alpha}}_{\text{NL Cancellation}} + \underbrace{\frac{y_d^{(v)} + \mathcal{K}(\xi)}{\alpha}}_{\text{Closed loop tracking}} \tag{17}$$

where the quantity $\xi = y_m - y_d$ is the tracking error and $\mathcal{K}(\xi)$ is a closed loop feedback controller. Usually, in order to control a first-order system we use $\mathcal{K}$ as a proportional gain and for a second-order stabilization $\mathcal{K}$ represent a proportional-derivative gain. We recognize in equation (17) the typical mathematical expression of a "nominal control" in the "flatness-based" control (see [32] for details) in which the non-linear terms $\hat{F}$ is summed with a closed loop tracking of a reference trajectory $t \to y_d(t)$.

Remark : In our study-case, a second order *Ultra-Local Model* (v=2) was chosen to represent each attitude dynamic of the MAV. It is important to emphasize that MFC algorithms have been developed to Single-Input Single-Output (SISO) systems and *MAVion* has been modeled by four inputs and ten outputs. Wherefore, a control architecture composed by multiple SISO MFCs, is proposed. Let's consider a single state dynamic, for example the pitch angle θ, that is controlled by symmetric flap deflections (δ_l,δ_r), see Figure 3. Thus, by analogy with equation (12) and from Figure 6, the *Ultra-Local Model* can be represented by the following equation :

$$\ddot{\theta} = F_\theta + \alpha_\theta \cdot \delta_e \tag{18}$$

From the general form of equation (17), the closed-loop can be computed by :

$$\delta_e = \frac{-\hat{F}_\theta + \ddot{\theta}_d + \mathcal{K}(\xi_\theta)}{\alpha_\theta} \tag{19}$$

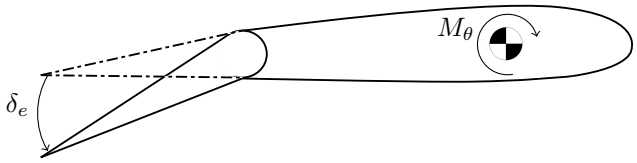

Fig. 6: Moment generated around *y-axis* by symmetrical flap deflections.

Substituting equation (19) in equation (18) with $\mathcal{K}$ equals to proportional-derivative gains, leads to :

$$\ddot{\theta} = F_\theta - \hat{F}_\theta + \ddot{\theta}_d + K_p\,\xi_\theta + K_d\,\dot{\xi}_\theta \tag{20}$$

It follows that theoretically, if the error (ξ_{F_θ}) between the pitch angle estimator ($\hat{F}_\theta$) and the real pitch angle dynamic (F_θ), is approximately zero during $[t-T, t]$:

$$\xi_{F_\theta} = F_\theta - \hat{F}_\theta \approx 0$$

The previous assumption allows us to simplify the equation (20) to equation (22).

$$\ddot{\xi}_\theta = \ddot{\theta} - \ddot{\theta}_d \tag{21}$$

$$\ddot{\xi}_\theta - K_p\,\xi_\theta - K_d\,\dot{\xi}_\theta = 0 \tag{22}$$

Combining all these results, the pitch angle and its dynamic error (ξ_θ) can be easily tuned by proportional and derivative gains, respectively K_p and K_d. The *NL Cancellation* term in equation (17), compensates the disturbances that could perturb the output state. Such an approach is easy and systematic for more complex dynamical systems than the ones represented in §II. Note that, a simple proportional-derivative controller is enough to ensure convergence of the error to zero. Such integration effect is implicitly involved in the model-free control.

The same steps from equation (18) to equation (22) have been done to control the forward speed in order to assure the flight stability during the transitioning flight. The MFC parameters that were used in this preliminary study are shown in the Table II.

TABLE II: MFC parameters

Gains	Pitch angle (θ)	Forward speed
T	6	5
α	850	4000
Kp	5	2
Kd	5	2

IV. SIMULATION FLIGHT AND ANALYSIS

We now illustrate the control performance reached by the scheduled-LQR and MFC during a transitioning flight, both strategies were used to stabilize the tail-sitter model described in §II-B. The simulation is discretized at 500 Hz and includes additional sensor noises, state estimation errors and wind disturbances around 4 m/s (w_u, w_w), as we can see in Figure 8f. Wind disturbances are imposed along x and z axes in order to disturb the pitch angle, especially during the transition phase. Propeller speed saturation is set at 1000 (rad/s) and flap deflections are saturated at 30 degrees, however they are not reached as can be seen in Figure 8d and 8e, respectively. In Figure 8a, the flight path describes a vertical take-off, followed by transitioning flight and the simulation ends when the aircraft is stabilized in forward flight mode. Transition from hovering to forward flight is triggered and controlled by means of desired forward speed, which is zero in hovering mode. Transitioning flight is performed naturally by increasing desired forward speed. Both controllers work according to this strategy, but with small differences. Scheduled LQR uses a look-up-table with predefined trim points and knows the desired pitch angle which was predefined by means of wind-tunnel campaigns. MFC does not have any informations about the system or about trim points. In order to compute the pitch angle reference for transitioning phase, MFC uses a different control architecture in Figure 7, where the desired attitude, such as desired pitch angle, is computed by an outer-loop. This strategy allows us to define a singular and continuous controller with constant gains that is able to stabilize the entire flight envelope.

The vertical takeoff is realized at the beginning of the simulation (t ∈ [0;5]) where the propeller rotations, shown in Figure 8d, increase to reach a higher altitude. During hovering flight (t ∈ [5;18]), the aircraft is more susceptible to perturbations caused by horizontal wind (w_u). However, because of low forward speed, aerodynamic effects are predominantly caused by prop wash. In this phase of the flight, the prop wash is high and important due to high propeller rotations that generate thrust to equalize the weight force, in order to maintain a desired altitude. Despite pitch oscillations in Figure 8c due to winds, both controllers are able to stabilize the MAV and the control authority of both controllers is also sufficient to handle disturbances. However, LQR can not manage these disturbances as good as MFC. That implies oscillations in forward speed, as can be seen in Figure 8b, and position errors may result.

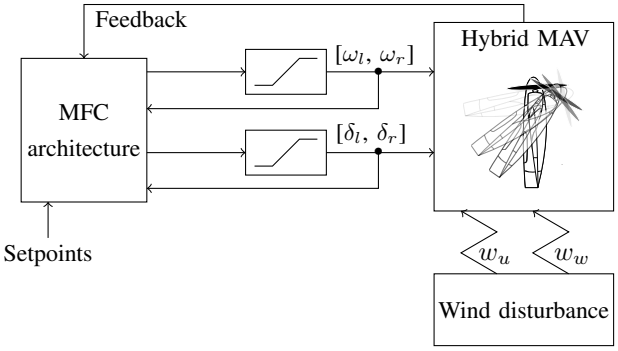

Fig. 7: MFC architecture designed for HMAVs with saturated control inputs. Propeller speeds (ω_l, ω_r) and flap deflections (δ_l, δ_r) are computed by means of *MFC architecture* block.

Figure 8c also clearly shows the pitch angle during the transitioning flight. The desired pitch angle trajectory computed by the LQR takes 5 seconds to perform the transition and MFC perform the transition in about 10 seconds. In this part of the flight (t ∈ [18;28]), both controllers ensured stability for pitch angle variation from hovering ($\theta = 90°$) to forward flight ($\theta \approx 10°$). In forward flight, a static error in the trajectory controlled by LQR is highlighted. This is visible especially at 30th seconds of simulation when wind disturbances are increased.

For comparison purposes, we evaluate the performance of both controllers, LQR and MFC, according to the following criterion :

$$RMSE_y = \sqrt{\frac{\sum_1^n (y - y_d)^2}{n}} \tag{23}$$

where n is the sample quantity. *Root Mean Square Error (RMSE)* is frequently employed in estimation to measure the differences between values predicted by an estimator and the values actually observed. Similarly, we propose to use this criterion to quantifies the error between the desired output reference and the measured value. The smaller the RMSE, the higher the controller performance. As the RMSE is sample-dependent, both control algorithms run at the same sampling frequency.

Table III shows the RMSE results for hovering flight mode (t ∈ [0;18]). We compute this criterion for pitch angle and for forward speed in disturbed flight conditions. MFC presents better robustness properties than LQR.

TABLE III: LQR vs MFC : RMSE - Hovering flight

y	Scheduled LQR	MFC	SI Units
Pitch angle (With wind)	4.8131	3.2893	[°]
Forward speed (With wind)	0.3170	0.2293	[m/s]

In Table IV, the performance of both controllers is demonstrated for the entire flight envelope : hovering, transition and forward flight (t ∈ [0;50]). Firstly, RMSE was computed for pitch angle and for forward speed in calm conditions (No wind). Secondly, the RMSE was computed in disturbed flight conditions (With wind).

TABLE IV: LQR vs MFC : RMSE - Entire flight envelope

y	Scheduled LQR	MFC	SI Units
Pitch angle (No wind)	3.0646	1.5131	[°]
Forward speed (No wind)	0.8699	1.4613	[m/s]
Pitch angle (With wind)	4.5357	2.7858	[°]
Forward speed (With wind)	1.8349	1.4700	[m/s]

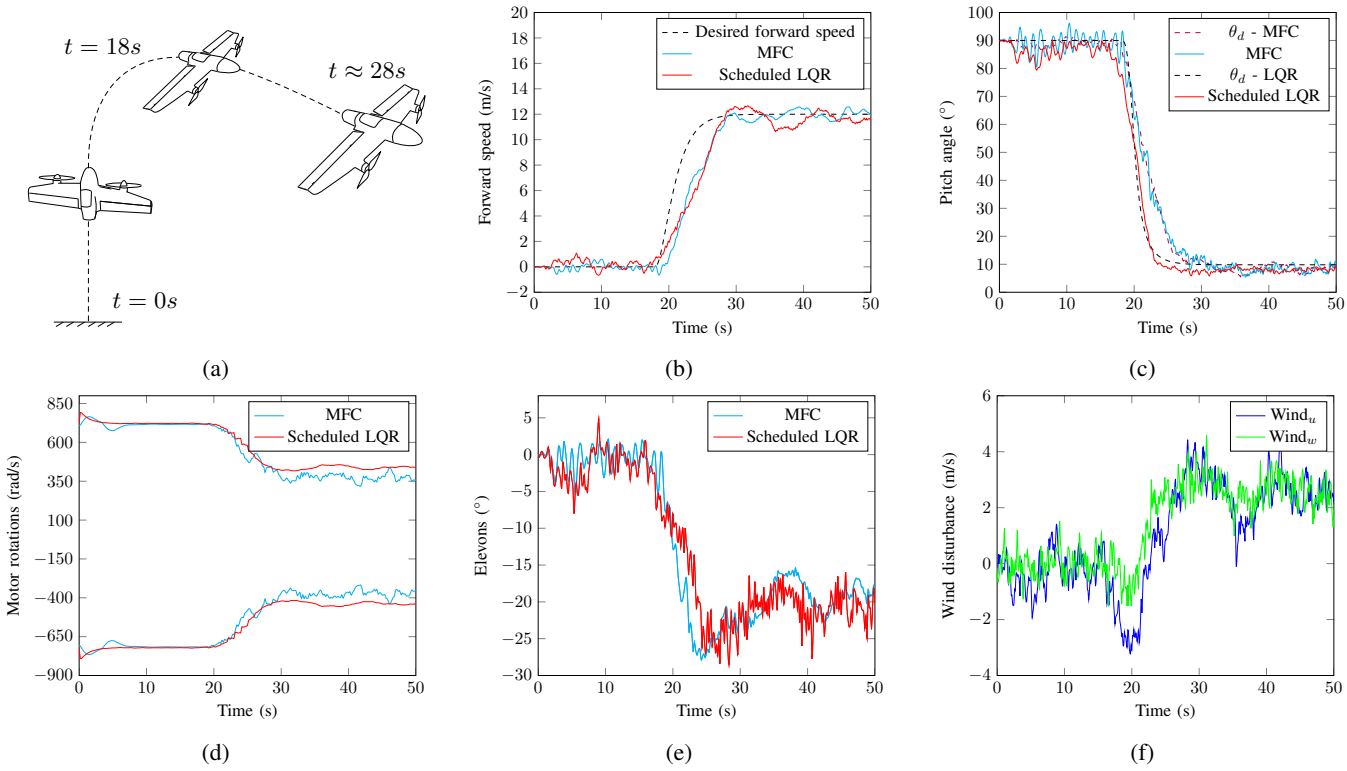

Fig. 8: Transition flight tests. On the top, from left to right: Flight path, forward-speed and pitch angle. On the bottom: propeller speeds ($\omega_l < 0$ and $\omega_r > 0$) due to counter-rotation sense, elevon deflections (δ_l and δ_r) convention negative for pitch-up, and wind disturbance along x and z axes.

Fig. 9: Cyclone MAV.

It can be concluded that LQR approach performed a better velocity tracking than MFC for simulations without wind. On the other hand, MFC exhibited strong disturbance-rejection properties in windy conditions for hovering and forward flight, and for the transitioning between both. Thus, the new control strategy employed herein which is based on the properties of MFC ensures a stable flight during the hovering-to-forward trajectory. Furthermore, MFC is able to control an unmodeled and under-actuated system despite all aerodynamic-coefficients alterations due to variations in angle of attack and control effectiveness.

The performance of the proposed control architecture based on MFC algorithms is shown through numerical simulation during hovering, transitioning and forward flight for a generic HMAV. The next steps consist to implement this control architecture in a new HMAV whose aerodynamic characteristics were improved, such as the *Cyclone* shown in Figure 9. Therefore, we will be able to study more precisely the MFC's adaptability.

V. CONCLUSION

This preliminary study proposed a potential method for designing controllers without any knowledge of the MAV. Initial results of attitude and velocity control using MFC for a Fixed-Wing MAV with transitioning flight capabilities, are presented. Simulation results showed a better attitude control obtained by MFC, both with wind or without wind. The flight velocity is controlled more accurately with scheduled LQR when there is no wind, however MFC showed a better performance when there is uncertainty in the environment, such as wind. This demonstrates the disturbance rejection and control of unmodeled dynamics with MFC by the means of its adaptive properties. Overall, MFC demonstrates a promising performance over LQR, and can be used for unconventional configurations such as tail-sitters, as well as during the unmodeled flight phases such as post-stall.

VI. FUTURE WORK

Further research is required to analyze the MFC properties in detail, such as exhaustive comparative studies between MFC, nonlinear control approaches and adaptive control

technique. MFC algorithms are being implemented in *Paparazzi* open-source autopilot system (cf. Paparazzi project at: `https://wiki.paparazziuav.org/`) and experimental flights will be presented soon.

REFERENCES

[1] M. Bronz, E. J. J. Smeur, H. G. de Marina, and G. Hattenberger, "Development of A Fixed-Wing mini UAV with Transitioning Flight Capability," *35th AIAA Applied Aerodynamics Conference, AIAA Aviation Forum*, (AIAA 2017-3739), June 2017.

[2] Adnan S. Saeed, Ahmad Bani Younes, Shafiqul Islam, Jorge Dias, Lakmal Seneviratne, Guowei Cai, "A Review on the Platform Design, Dynamic Modeling and Control of Hybrid UAVs," *International Conference on Unmanned Aircraft Systems (ICUAS)*, Denver, Colorado, USA, pp. 806-815, June 2015.

[3] Jason M. Beach, Matthew E. Argyle, Timothy W. McLain, Randal W. Beard and Stephen Morris, "Tailsitter Attitude Control Using Resolved Tilt-Twist," *International Conference on Unmanned Aircraft Systems (ICUAS)*, Orlando, FL, USA, May 27-30, 2014.

[4] E. J. J. Smeur, G. C. H. E. de Croon, and Q. Chu, "Cascaded Incremental Nonlinear Dynamic Inversion Control for MAV Disturbance Rejection," *Control Engineering Practice*, pp. 79-90, January 2018.

[5] J. Escareño, R. H. Stone, A. Sanchez and R. Lozano, "Modeling and Control Strategy for the Transition of a Convertible Tail-sitter UAV," *Proceedings of the European Control Conference*, Kos, Greece, July 2007.

[6] D. Pucci, T. Hamel, P. Morin and C. Samson, "Nonlinear Control of Aerial Vehicles Subjected to Aerodynamic Forces," *52nd IEEE Conference on Decision and Control*, December 10-13 2013.

[7] V. Martinez, O. Garcia, A. Sanchez, V. Parra, and A. Escobar, "Adaptive backstepping control for a convertible UAV," *Workshop on Research, Education and Development of Unmanned Aerial Systems (RED-UAS)*, November 23-25, 2015.

[8] P. Casau, D. Cabecinhas, and C. Silvestre, "Hybrid Control Strategy for the Autonomous Transition Flight of a Fixed-Wing Aircraft," *50th IEEE Conference on Decision and Control and European Control Conference (CDC-ECC)*, November 2013.

[9] P. Casau, D. Cabecinhas, and C. Silvestre, "Autonomous Transition Flight for a Vertical Take-Off and Landing Aircraft," *IEEE transactions on control systems technology*, Orlando, FL, USA, December 12-15, 2011.

[10] L. R. Lustosa, F. Defay, and J.-M. Moschetta, "Longitudinal study of a tilt-body vehicle: modeling, control and stability analysis," *International Conference on Unmanned Aircraft Systems (ICUAS)*, Denver, Colorado, USA, pp. 816-824, June 2015.

[11] L. R. Lustosa, J. M. O. Barth, J.-P. Condomines, F. Defay, and J.-M. Moschetta, "Team MAVion entry in the IMAV17 outdoor challenge A tail-sitting trajectory-tracking μUAV," *International Micro Air Vehicle Conference and Competition*, Toulouse, France, September 2017.

[12] D. Chu, J. Sprinkle, R. Randall, and S. Shkaraye, "Simulator development for transition flight dynamics of a vtol mav," *International Journal of Micro Air Vehicles*, 2(2):6989, 2010.

[13] E. J. J. Smeur, Q. Chu, and G. C. H. E. de Croon, "Adaptive Incremental Nonlinear Dynamic Inversion for Attitude Control of Micro Air Vehicles," *Journal of guidance, control and dynamics*, Vol. 39, No. 3, pp. 450-461, March 2016.

[14] T. P. Lillicrap, J. J. Hunt, A. Pritzel, N. Heess, T. Erez, Y. Tassa, D. Silver, and D. Wierstra, "Continuous control with deep reinforcement learning," *6th International Conference on Learning Representations*, Vancouver, 2016.

[15] M.-B. Radac, R. E. Precup, R. C. Roman, "Model-Free control performance improvement using virtual reference feedback tuning and reinforcement Q-learning," *International Journal of Systems Science*, 2017.

[16] M. Fliess, and C. Join, "Model-free control," *International Journal of Control, Taylor & Francis*, pp. 2228-2252, 2013.

[17] Ouassim Bara, M. Fliess, C. Join, Judy Daye, and Seddik M. Djouadi, "Toward a model-free feedback control synthesis for treating acute inflammation," *Journal of Theoretical Biology*, pp. 26-37, 2018.

[18] Younes AI Younes, Ahmad Drak, Hassan Noura, Abdelhamid Rabhi and Ahmed EI Hajjaji, "Model-Free Control of a Quadrotor Vehicle," *International Conference on Unmanned Aircraft Systems (ICUAS)*, Orlando, FL, USA, pp. 1126-1131, May 2014.

[19] N. O. Pérez-Arancibia, P.-E. J. Duhamel, K. Y. Ma, R. J. Wood, "Model-Free Control of a Hovering Flapping-Wing Microrobot," *Journal of Intelligent & Robotic Systems*, pp. 95-111, January 2015.

[20] Aneesh N. Chand, Michihiro Kawanishi, Tatsuo Narikiyo, "Non-linear model-free control of flapping wing flying robot using iPID," *IEEE International Conference on Robotics and Automation (ICRA)*, May 2016.

[21] Younes Al Younes, Ahmad Drak, Hassan Noura, Abdelhamid Rabhi and Ahmed El Hajjaji, "Robust Model-Free Control Applied to a Quadrotor UAV," *Journal of Intelligent & Robotic Systems*, pp. 37-52, December 2016.

[22] Haoping Wang, Xuefei Ye, Yang Tian, Gang Zheng, and Nicolai Christov, "Model-FreeBased Terminal SMC of Quadrotor Attitude and Position," *IEEE Transactions on Aerospace and Electronic Systems*, Vol. 52, pp. 2519 - 2528, October 2016.

[23] Gabriele Di Francesco and Massimiliano Mattei, "Modeling and Incremental Nonlinear Dynamic Inversion Control of a Novel Unmanned Tiltrotor," *Journal of Aircraft*, 2015.

[24] Haowei Gu, Ximin Lyu, Zexiang Li, Shaojie Shen, and Fu Zhang, "Development and Experimental Verification of a Hybrid Vertical Take-Off and Landing (VTOL) Unmanned Aerial Vehicle (UAV)," *International Conference on Unmanned Aircraft Systems (ICUAS)*, Miami, FL, USA, June 13-16, 2017.

[25] J. L. Forshaw, V. J. Lappas, and P. Briggs, "Transitional Control Architecture and Methodology for a Twin Rotor Tailsitter," *Journal of Guidance, Control and Dynamics*, Vol. 37, No. 4, JulyAugust 2014.

[26] J. L. Forshaw, and V. J. Lappas, "High-Fidelity Modeling and Control of a Twin Helicopter Rotor Tailsitter," *AIAA Guidance, Navigation, and Control Conference*, August 2011, Portland, Oregon, 2011.

[27] Gerardo Flores and R. Lozano, "Transition Flight Control of the Quad-Tilting Rotor Convertible MAV," *International Conference on Unmanned Aircraft Systems (ICUAS)*, pp.789-794, 2013.

[28] Christos Papachristos, Kostas Alexis and Anthony Tzes, "Hybrid Model Predictive Flight Mode Conversion Control of Unmanned Quad-TiltRotors," *European Control Conference (ECC)*, pp.1793-1798, July 17-19, Zürich, Switzerland, 2013.

[29] L. R. Lustosa, F. Defay, and J.-M. Moschetta, "A global singularityless polynomial-like aerodynamics model for algorithmic flight control of tail-sitters," *AIAA Journal of Guidance, Control, and Dynamics* (to appear).

[30] L. R. Lustosa, F. L. Cardoso-Ribeiro, F. Defay, and J.-M. Moschetta, "A new look at the uncontrollable linearized quaternion dynamics with implications to LQR design in underactuated systems," *European Control Conference*, 2018.

[31] J. Zehetner, J. Reger, and M. Horn, "A Derivative Estimation Toolbox based on Algebraic Methods - Theory and Practice," *2007 IEEE International Conference on Control Applications*, pp. 331-336, Singapore, 2007.

[32] M. Mboup, C. Join, and M. Fliess, "A revised look at numerical differentiation with an application to nonlinear feedback control," *In 15th Mediterranean conference on Control and automation (MED'07)*, Athenes, Greece, 2007.